

Fourfold Anisotropic Magnetoresistance and Unconventional Critical Exponents in Twinned FePd_2Te_2

Zhaoxu Chen

*Beijing National Laboratory for Condensed Matter Physics,
Institute of Physics, Chinese Academy of Sciences, Beijing 100190, China and
School of Physical Sciences, University of Chinese Academy of Sciences, Beijing 100049, China*

Yuxin Yang

*Beijing National Laboratory for Condensed Matter Physics,
Institute of Physics, Chinese Academy of Sciences, Beijing 100190, China and
College of Materials Sciences and Opto-Electronic Technology,
University of Chinese Academy of Sciences, Beijing 100049, China*

Jian-gang Guo*

*Beijing National Laboratory for Condensed Matter Physics,
Institute of Physics, Chinese Academy of Sciences, Beijing 100190, China*

As a special material symmetry operation, crystal twins usually influence physical properties. Here, detailed electrical transport and magnetic measurements were performed to reveal twinning effect on properties of van der Waals ferromagnet FePd_2Te_2 . Orthorhombic crystal domains were observed in polarized optical microscopy and fixed $\pi/2$ angle between adjacent domains suggests a phase transition origin of the twins. FePd_2Te_2 exhibits fourfold in-plane anisotropic magnetoresistance. It is attributed to antiferromagnetic coupling component near atomically flat twin boundary and pseudo four-fold symmetry from perpendicular Fe chains. Intense magnetic domain motion is suggested by Hopkinson effect observed in magnetic susceptibility. A set of unusual critical exponents $\beta = 0.866$, $\gamma = 1.043$, $\delta = 2.20$ cannot be classified in any universal class predicted by renormalized group. Deviation from standard model reflects the non-saturating magnetization and slow growth of spontaneous magnetization resulting from crystal domain walls. These results show that additional symmetry from twins and twin boundary have a significant effect on electrical transport and magnetic properties of FePd_2Te_2 . There is much room to modulate physical properties of twinned van der Waals ferromagnets through twins.

I. INTRODUCTION

A twinned crystal is an aggregate in which domains with different orientations growth together according to symmetry operation described by twin laws[1]. Crystal twins can be generated by a solid state phase transition, an external force or a perturbation during the crystal growth[2]. For crystal twins generated by the latter two random factors, the symmetry relation between different domains cannot be given a prior orientation[2]. Whereas, phase-transition-driven crystal twinning effect is more interesting and has been studied deeply in strong correlated systems[3]. For example, in ferroelastic-like tetragonal-to-orthorhombic transition during cooling, C_4 is lost as a point group symmetry operation. To minimize the elastic and release strain, twin domain structures form. Such orthorhombic domains have been widely observed in unconventional superconductors and related materials with tetragonal-to-orthorhombic phase transformation, such as $\text{YBa}_2\text{Cu}_3\text{O}_{7-\delta}$ [4], $\text{La}_{2-x}\text{Sr}_x\text{CuO}_4$ [5], AFe_2As_2 ($A = \text{Ca/Sr/Ba/Eu}$)[6] and Co-doped counterpart[7], NaFeAs [8] and FeSe [9].

Although crystal twins is only a structural concept, it has significant effect on physical properties. In supercon-

ductors, as a kind of defects, domain walls between adjacent twins can effectively pin the vortices and increase the critical current density[10–12]. In terms of superconducting mechanisms, twin boundaries can invoke twist of the order parameter structure and breaks time-reversal symmetry[13, 14]. Besides, in Fe-based superconductors, coupling between twins and magnetism has been deeply studied in the anisotropy of in-plane resistivity, charge dynamics and electronic structure[3]. Compared with these strong correlated materials and conventional magnetic films, due to the lack of twinned bulk counterpart, study on interplay between twinning effect and van der Waals ferromagnet is not carried out yet. Recent discovered van der Waals ferromagnet FePd_2Te_2 with $T_c \sim 180$ K crystallize in a monoclinic space group $P2_1/m$ and exhibit a layered structure along [10-1] direction[15]. Within cleavage plane, perpendicular Fe chains lead to orthorhombic twins with size of ~ 100 nm[15].

Here, we report the twinning effect on electrical transport and magnetic properties of FePd_2Te_2 . AC and DC magnetic susceptibility measurements reveal the paramagnetic-to-ferromagnetic transitions, which is also evidenced by anomalous Hall effect and temperature-dependent resistance. Anisotropic magnetoresistance was performed to investigate the twin-induced in-plane anisotropy and four-fold symmetry was discovered. It is noted that the in-plane anisotropic magnetoresistance

* jgguo@iphy.ac.cn

can be modulated by strain introduced by extra Pd atoms. Critical exponents were calculated through detailed magnetic properties as $\beta = 0.866$, $\gamma = 1.043$, $\delta = 2.20$. These results confirmed the decouple between the dimensionality of quasi-one-dimensional Fe chain and that of mean-field-like magnetism, emphasizing the importance of crystal twins and twin boundary.

II. EXPERIMENTAL METHODS

FePd₂Te₂ single crystals were grown by congruent melting. Fe, Pd and Te powder were weighted with a molar ratio of 1:2:2. The starting materials were loaded into alumina crucibles and sealed in an evacuated quartz tube. The sealed quartz tube was held at 800 °C for 24 h was cooled down to 550 °C within 8640 minutes. Finally, the crystals were annealed for long time and quenched in water. For FePd_{2.08}Te₂ single crystals, the growth method was similar.

X-ray diffraction was performed on a Rigaku Diffractometer with a Cu K_α anode (1.5418 Å) at room temperature. The DC magnetic susceptibility and initial isothermal magnetization were measured on a Magnetic Property Measurement System (MPMS, Quantum Design). AC magnetic susceptibility was measured on Physike system. The electrical transport was measured by a Physical Property Measurement System (PPMS Dynacool, Quantum Design) and Physike TKMS based on Keithley 6221/2182A and Stanford Research System Model SR830 DSP lock-in amplifier. The angular dependence of the magnetoresistance is determined within a 270° range under a magnetic field of 9 T.

III. RESULTS AND DISCUSSIONS

Figure 1(a) shows the X-ray diffraction pattern of a typical annealed FePd₂Te₂ single crystal indexed by ($h0-h$) Miller indices. Polarized microscopy is a useful tool to observe crystal domains directly. Figure 1(b) exhibits the optical image obtained through polarized microscopy. It is noted that there are perpendicular stripes on the surface, which originate from crystal domain observed in previous scanning tunneling microscopy[15]. The twins in FePd₂Te₂ should be classified as transformation twins rather than mechanical/growth twins. Mechanical/growth twins result from random factors including external force and perturbation induced coalescence of micro-crystals, so their relative orientations are also random and cannot be predicted. Transformation twins are driven by solid state phase transition during which some specific point symmetry operations in high-symmetry phase at high temperature are lost in low-temperature phase with low symmetry, so the orientation can be predicted and are fixed[2]. The perpendicular crystal domains in FePd₂Te₂ indicate that there is a possible orthorhombic-to-monoclinic phase transition, which was ever observed in Bi₂Sr₂CaCu₂O_y and need

further study[16].

As shown in Fig. 1(c), temperature-dependent of Hall effect exhibits hysteresis at low temperature, which evidences the presence of ferromagnetic phase. The paramagnetism to ferromagnetism transition is also observed in temperature-dependent resistance in Fig. 1(d). The kink indicates that the critical temperature is ~ 180 K. Inset is AC magnetic susceptibility with no DC bias magnetic field. The peak corresponds to the phase transition at 184 K. It is noted that real part of AC susceptibility for a ferromagnet below T_c is expected to be a constant down to low temperatures theoretically with freezing out of domain wall dynamics[17–20]. However, peak is also observed in many amorphous alloys[21] and inhomogeneous phase-separated magnetic systems with small size of ferromagnetic and antiferromagnetic clusters[22–24]. It is attributed to Hopkinson effect[25], which reflects the competition between thermo-magnetic randomization (magnetic anisotropy) and domain boundary expansion[26], suggesting the intense magnetic domain motion.

In Fig. 1(e), AC magnetic susceptibility with a series of DC bias magnetic field from 50 to 1000 Oe was employed to investigate the magnetic properties of FePd₂Te₂. Upon increasing DC bias magnetic field, the real part peak of AC magnetic susceptibility becomes broader with reduced peak value. With zero and small DC field, the peak moves to low temperature. When the DC field reaches as high as ~ 250 Oe, the peak splits into two maxima, as shown in the inset of Fig. 2(e). Further increasing DC bias field moves the first maximum to low temperature, while the other to high temperature, as indicated by the dash line. When DC bias field exceeds 450 Oe, the first peak almost vanishes. This phenomena was ever observed in other ferromagnetic systems[21, 27]. The first peak is closely related to the magnetization process including domains, hysteresis, nonuniform magnetostatic modes, etc, while the second peak corresponds to the critical fluctuation[27]. The evolution of the first peak is in accord with that expected for Hopkinson effect, i.e., increases rapidly below T_c , and decreases and shifts to lower temperature with increasing small dc field[21]. As a result, the actual peak at zero-field contains two parts of contribution from Hopkinson effect and critical fluctuation, respectively. In principle, AC susceptibility can be used to calculate critical exponents[21]. Because it is hard to distinct the peak from critical fluctuation from Hopkinson effect, effort to analyze critical behavior from AC susceptibility was failed.

Figure 2(a) shows the magnetoresistance of FePd₂Te₂ under H along [10-1], i.e., out-of plane. Upon temperature decreases below T_c , the shape of low-field magnetoresistance change from dome-like, peak-like to butterfly-shaped hysteresis, indicating the emergence of ferromagnetism. To explore the effect of crystal twins on in-plane electrical transport, we measured in-plane anisotropic magnetoresistance under 9 T at different temperatures as shown in Fig. 2(b)-(j). There is no anisotropy within resolution at high temperature exceeding 230 K. When

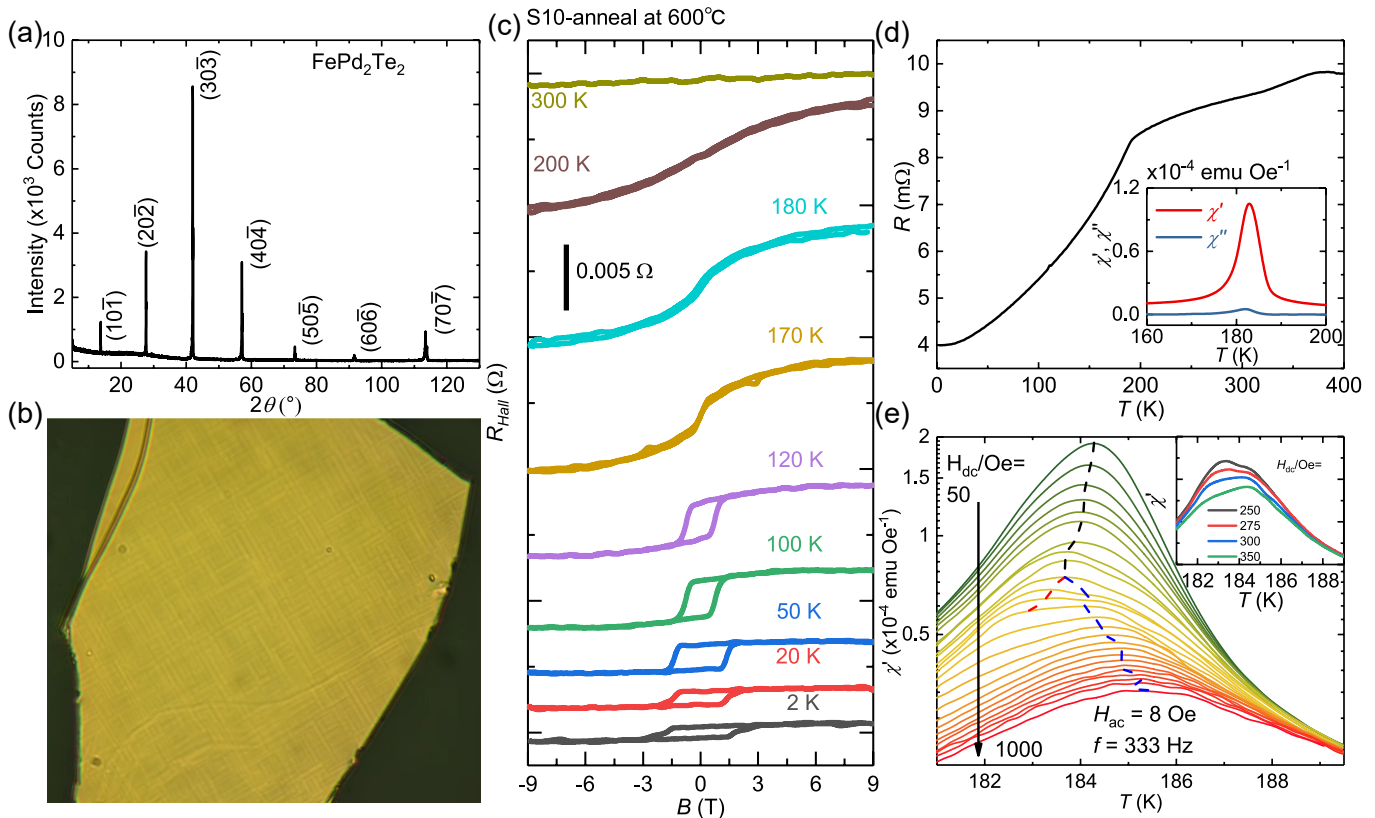


FIG. 1. Structure characterization and basic physical properties. (a) X-ray diffraction of a FePd_2Te_2 single crystal. (b) Observation of orthorhombic crystal domain caused by twinning effect through optical microscopy. (c) Anomalous Hall effect of an annealed FePd_2Te_2 single crystal. (d) Temperature-dependent resistance of FePd_2Te_2 single crystal. Inset is AC magnetic susceptibility with $H_{ac} = 4$ Oe and $f = 333$ Hz. (e) AC magnetic susceptibility with $H_{ac} = 4$ Oe and $f = 333$ Hz under a series of DC bias magnetic field from 50 Oe to 1000 Oe. Inset is enlarged plot of AC magnetic susceptibility under several selected DC bias magnetic field.

temperature decreases to 200 K slightly higher than T_c , there is a pair of strong peaks when magnetic field is perpendicular to current. Also, two weak peaks appear when magnetic field is parallel to current. Upon temperature decreases, intensity of the weak peaks become stronger and gradually exceed that of the other pair.

Generally, anisotropic magnetoresistance is usually two-fold symmetric, which is explained by spin-orbit coupling traditionally. High resistance state emerge with $H \parallel I$, while low resistance state with $H \perp I$. Besides contribution from ordinary magnetoresistance, anisotropic magnetoresistance usually reflects the anisotropic Fermi surface and charge-spin interactions[28]. In magnetic materials, it can be described by

$$\rho_{xx} = \rho_{\perp} + (\rho_{\parallel} - \rho_{\perp}) \cos^2 \theta_M, \quad (1)$$

where θ_M is the angle between magnetization and current. Because obvious anisotropy starts from ~ 200 K, anisotropic magnetoresistance in FePd_2Te_2 is closely related to long-range magnetic order below T_c and strong magnetic fluctuation above T_c , respectively. It is also noted that anisotropic magnetoresistance in FePd_2Te_2 exhibit a four-fold symmetry. Such high order

anisotropy magnetoresistance is also observed in other magnetic materials including magnetic films[29], antiferromagnetic cuprate with twins[30] and van der Waals ferromagnets[31]. It is usually attributed to magnetic anisotropy[32, 33], relaxation time anisotropy[34], spin-dependent scattering near antiphase boundary[30, 35] and lattice symmetry[29].

Anisotropic magnetoresistance of FePd_2Te_2 in Fig. 2(b)-(j) was collected under field as high as 9 T. Such a high field is enough to align the magnetic moments along the direction of the field and subsequently exclude the possibility of magnetic anisotropy. This is also suggested by the fact that the peak of anisotropic magnetoresistance occurs along the direction $H \parallel I$ rather than $M \parallel I$. Aligned magnetic moments make direction of H and M equivalent. Considering the twinning effect, the high-order anisotropic magnetoresistance should be closely related to the pseudo four-fold lattice symmetry induced by perpendicular Fe chains. Twin boundary is also needed to be considered. In epitaxial Fe_3O_4 films[36, 37] and high T_c cuprates[30], four-fold anisotropic magnetoresistance is attributed to antiphase antiferromagnetic domain boundaries[35]. This physical picture of spin-polarized transport across sharp antiferromagnetic boundaries also

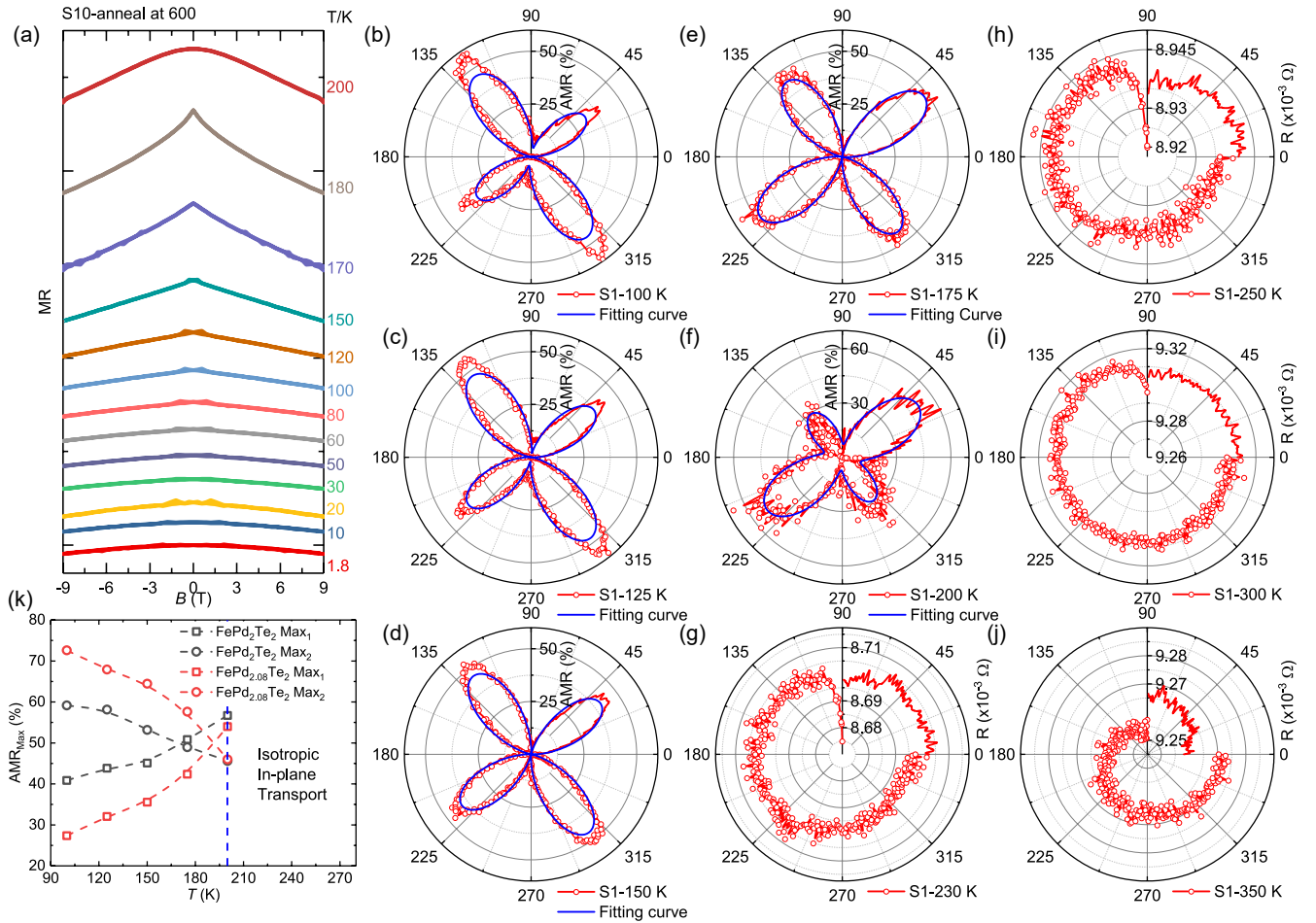


FIG. 2. Anisotropic in-plane electrical transport. (a) Magnetoresistance of $FePd_2Te_2$ single crystal with $H // [10-1]$ from 1.8 to 200 K. (b-j) Polar plot of anisotropic in-plane magnetoresistance under a magnetic field of 9 T from 100 K to 350 K. An extra four-order term was used to fit the data. The fitting curves are blue. (k) Temperature-dependent of ratio between the two maxima in the in-plane magnetoresistance.

applies to $FePd_2Te_2$. In $FePd_2Te_2$, magnetic moments near crystal domain boundary of orthorhombic twins with in-plane anisotropic Fe chains can be naturally resolved ferromagnetic and antiferromagnetic components at zero field[15]. At low fields, moments in discrete twins are gradually aligned along the direction of H . At high field, the moments near twin boundary components coupled with antiferromagnetism start to align along H . This also leads to additional high-order contribution in anisotropic magnetoresistance. High-field four-fold anisotropic magnetoresistance in $FePd_2Te_2$ is quite similar to Fe_3O_4 [36], and is opposite to magnetite films[32, 33]. Low-field anisotropic magnetoresistance is still needed for further analysis. Also, spin-polarized transport across sharp antiferromagnetic boundaries results to non-saturating magnetization[37] and linear magnetoresistance[35], which has been observed in $FePd_2Te_2$ and evidenced by critical exponents obtained below. Since four-fold anisotropic magnetoresistance corresponds to pseudo four-fold symmetry from perpendicular Fe chains and resulting atomic sharp twin boundary with partially antiferromagnetic

coupling, the additional four-fold anisotropic magnetoresistance should be able to be modulated by the fraction of twin boundaries. Figure 2(k) shows the value of two sets of anisotropic magnetoresistance peaks of $FePd_2Te_2$ and $FePd_{2.08}Te_2$, respectively. Strain from 4% Pd atoms influence the crystal twins and subsequently changes anisotropic magnetoresistance successfully.

Besides the influence of crystal twins on electrical transport, detailed measurements were performed to investigate the effect on magnetic properties in $FePd_2Te_2$. Figure 3(a) shows the magnetic susceptibility under 1000 Oe with $H // c$ -axis. A ferromagnetic-paramagnetic magnetic transition occurs around 180 K. Curie-Weiss fitting gives a effective moment μ_{eff} with $3.9 \mu_B$. Besides, a downturn was observed in χ^{-1} at around 200 K, corresponding to the starting temperature of anisotropic magnetoresistance. A Hopkinson peak was observed just below T_C . Such obvious Hopkinson peak is rather rare in other van der Waals ferromagnets, so twinning effect may cause more complex magnetic domains in $FePd_2Te_2$.

Initial isothermal magnetization along c -axis near T_C was measured and shown in Fig. 3(b). Arrott-Stokes

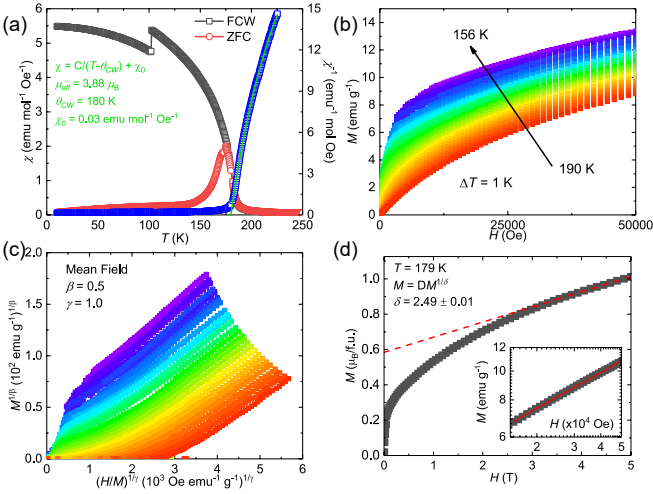


FIG. 3. Magnetic Properties and entropy change. (a) Temperature-dependent magnetic susceptibility and reverse magnetic susceptibility along $H//c$ -axis. Black, red and blue lines represent zero-field-cooling, field-cooling-warming magnetic susceptibility and reverse magnetic susceptibility, respectively. The anomaly around 100 K is a break-point due to measurement error. (b) Initial isothermal magnetization along $H//c$ -axis near Curie temperature. (c) Arrott plot of M^2 vs H/M . (d) Initial isothermal magnetization at 179 K for FePd₂Te₂ along $H//c$ -axis. The saturated magnetic moment is $0.58 \mu_B$. Inset is log-log scale with a fitting curve.

equations are usually employed to analyze the critical behaviors of a magnetic phase transition as below[38],

$$\left(\frac{H}{M}\right)^{1/\gamma} = a\varepsilon + bM^{1/\beta}, \quad (2)$$

where ε is reduced temperature $\varepsilon = (T - T_c)/T_c$, and a and b are constants. Six different kinds of theoretical models with short-range interactions were used to construct the modified Arrott plots, which are mean field model ($\beta=0.5$, $\gamma=1.0$), tricritical mean field model ($\beta=0.25$, $\gamma=1.0$), 3D Heisenberg model ($\beta=0.365$, $\gamma=1.386$), 3D XY model ($\beta=0.345$, $\gamma=1.316$), 3D Ising model ($\beta=0.325$, $\gamma=1.24$), 2D Ising model ($\beta=0.125$, $\gamma=1.75$). The mean field model was shown in Fig. 3(c), while the others in Supporting Information. In general, the normalized slope is a criterion to judge whether the model is appropriate. It is defined as $\text{slope}(T)/\text{slope}(T_c)$, where $\text{slope}(T) = dM^{1/\beta}/d(H/M)^{1/\gamma}$. If the theoretical model is appropriate, the temperature-dependent normalized slope should be equal to 1. Figure S1 gave the temperature dependence of normalized slope. Both above T_c and below T_c , mean field model was the most appropriate. However, it was found that T_c obtained from conventional Arrott plot did not match real T_c well, which suggest mean field model was not accurate enough.

Firstly, δ was fitted from equation,

$$M = DH^{1/\delta}, T = T_c, \quad (3)$$

where D is critical amplitudes[39]. Figure 3(d) shows the initial isothermal magnetization at T_c . δ was obtained

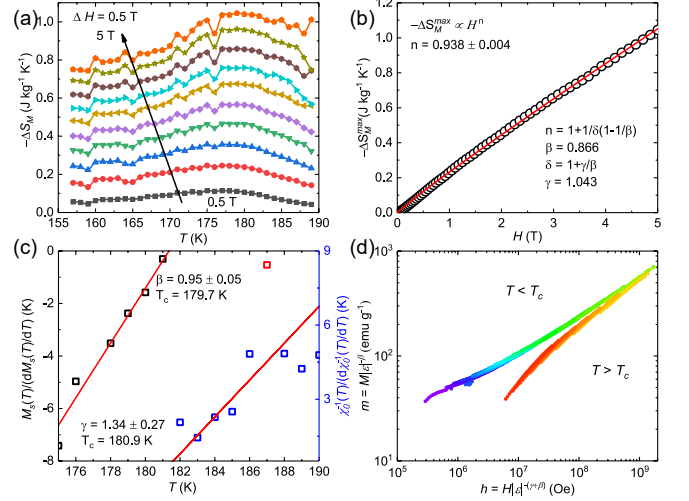


FIG. 4. Critical behavior and scaling analysis. (a) The magnetic entropy change $-\Delta S_M$ obtained from initial isothermal magnetization with $H//c$ -axis. (b) Field-dependence of the maximum magnetic entropy change $-\Delta S_M^{max}$. (c) Kouvel-Fisher plots, temperature dependence of $M_S(dM_S/dT)^{-1}$ (left axis) and $\chi_0^{-1}(d\chi_0^{-1}/dT)^{-1}$. Solid line represents fitting curve. (d) Scaling plot of renormalized magnetization m vs renormalized magnetic field h in log-log scale below and above T_c at high-field region.

as 2.49 ± 0.01 from the log-log scale in the inset of Fig. 3 (d), i.e., $\ln M = 1/\delta \ln h + \ln D$.

The magnetic entropy change also suggests the critical exponents of magnetic phase transition, which is closely related to the intrinsic magnetic coupling in FePd₂Te₂. Based Maxwell's relation, the magnetic entropy change is

$$\Delta S_M(T, H) = \int_0^H \left(\frac{\partial S}{\partial H}\right)_T dH = \int_0^H \left(\frac{\partial M}{\partial T}\right)_H dH. \quad (4)$$

According to above equation, Fig. 4(a) showed the calculated magnetic entropy change $-\Delta S_M(T, H)$ as a function of temperature under several magnetic fields along c -axis. All $-\Delta S_M(T, H)$ curves exhibit a peak at T_c . The maxima negative magnetic entropy change $-\Delta S_M(T, H)$ reached $1 \text{ J kg}^{-1} \text{ K}^{-1}$, which is at the same order of magnitude as other van der Waals magnets[40]. In Fig. 4(b), field-dependent $-\Delta S_M^{max}$ was fitted by

$$-\Delta S_M^{max} = aH^n \quad (5)$$

The fitting result gave $n=0.938(4)$. There is relation among n , δ , β , γ ,

$$n = 1 + \frac{1}{\delta} \left(1 - \frac{1}{\beta}\right), \quad (6)$$

$$\delta = 1 + \frac{\gamma}{\beta}, \quad (7)$$

Combining $\delta = 2.49 \pm 0.01$, β and γ was calculated as 0.866 and 1.043, respectively. New δ was calculated as 2.20 through Eq. (6).

TABLE I. Critical exponents of FePd₂Te₂ and different theoretical models

Composition	Technique	β	γ	δ
FePd ₂ Te ₂	Critical isotherm			2.49(1)
	Magnetic entropy analysis	0.87	1.04	2.20
	Kouvel-Fisher method	0.95(5)	1.34(3)	2.41(2)
Mean field	Theory	0.5	1.0	3.0
Tricritical mean field	Theory	0.25	1.0	5
3D Heisenberg	Theory	0.365	1.386	4.8
3D XY	Theory	0.345	1.316	4.81
3D Ising	Theory	0.325	1.24	4.82
2D Ising	Theory	0.125	1.75	15

We tried to get precise critical exponents through iterative method of modified Arrott plot[41], but it always diverged and got a T_c beyond the temperature range measured. So, similar values from magnetic entropy analysis were employed to construct modified Arrott plot $M^{1/\beta}$ vs $(H/M)^{1/\gamma}$ with $\beta = 0.87$ and $\gamma = 1.29$. Spontaneous magnetization M_S and inverse magnetic susceptibility χ_0^{-1} are obtained from the intercepts with the axis $M^{1/\beta}$ and $(H/M)^{1/\gamma}$ in the constructed modified Arrott plot. Through the temperature-dependent M_S and χ_0^{-1} , the Kouvel-Fisher method is used to determined the critical exponents[42],

$$\frac{M_S(T)}{dM_S(T)/dT} = \frac{T - T_c}{\beta}, \quad (8)$$

$$\frac{\chi_0^{-1}(T)}{d\chi_0^{-1}(T)/dT} = \frac{T - T_c}{\gamma}. \quad (9)$$

The results are shown in Fig. 4(c), giving $\beta = 0.95 \pm 0.05$ with $T_c = 179.7$ K and $\gamma = 1.34 \pm 0.27$ with $T_c = 180.9$ K, respectively. These results are close to the value calculated from magnetic entropy change analysis. Another samples were used to analyze the critical exponents, and the critical exponents obtained in these two processes are similar.

Besides cross validation by isothermal magnetization analysis at T_c , magnetic entropy change analysis and Kouvel-Fisher method, scaling analysis is also used to identify the reliability of critical exponents. The rescaled magnetization and rescaled magnetic field are defined as

$$m = \varepsilon^{-\beta} M(H, \varepsilon), \quad (10)$$

$$h = \varepsilon^{-(\beta+\gamma)} H, \quad (11)$$

where ε is reduced temperature. The magnetic equation of state in the critical region is

$$m = f_{\pm}(h). \quad (12)$$

This means that with right critical exponents, h -dependent m will be collapsed into two curves above and below T_c , respectively. In Fig. 4(d), two branches are observed clearly, which verifies the reliability of the obtained critical exponents.

Table I lists critical exponents of FePd₂Te₂ and different theoretical models with short-range interactions. Due to relatively large error bar in critical exponents obtained through Kouvel-Fisher method, the following discussions are based on those obtained by magnetic entropy analysis. In order to clarify the relation between crystal structure and magnetic coupling, we try to solve the space dimensionality d and spin dimensionality n of FePd₂Te₂. According to renormalization group analysis[43], the interactions between spins decay with spin-spin distance r as $J(r) \sim r^{-(d+\sigma)}$, where d is the space dimensionality and σ is constant. $\sigma > 2$ suggests a Heisenberg-type short-range interactions, corresponding to the theoretical models in Table I. It is obvious that magnetic coupling in FePd₂Te₂ cannot be described by any model with short-range interactions, i.e., $\sigma > 2$.

When σ lies between $d/2$ and 2, the interactions cannot be described by single type short- or long-range model. This also induces a continuous change of critical exponent γ . Almost all van der Waals magnets are located in this region[40]. In this case, the critical exponent γ is predicted as[43]

$$\gamma = 1 + \frac{4n+2}{dn+8} \Delta\sigma + \frac{8(n+2)(n-4)}{d^2(n+8)^2} \times \left(1 + \frac{2G(d/2)(7n+20)}{(n-4)(n+8)}\right) \Delta\sigma^2, \quad (13)$$

where

$$\Delta\sigma = (\sigma - d/2), \quad (14)$$

$$G(d/2) = 3 - 1/4 \times (d/2)^2. \quad (15)$$

We adjusted σ and different sets of $\{d:n\}$ to yield a value for γ close to that experimentally observed, i.e., $\gamma = 1.043$. The obtained σ can be use to calculate other critical exponents through following equations,

$$v = \gamma/\sigma, \quad (16)$$

$$\alpha = 2 - vd, \quad (17)$$

$$\beta = (2 - \alpha - \gamma)/2, \quad (18)$$

$$\delta = 1 + \gamma/\beta. \quad (19)$$

However, with γ closest to that experimentally observed, β and δ do not match corresponding experimental values.

These results inspired us to reconsider the magnetic coupling from a perspective of pure long-range interactions, i.e., $\Delta\sigma = \sigma - d/2 < 0$. In this regime, the exponents are calculated as below[43],

$$\gamma = 1, \quad (20)$$

$$\eta = 2 - \sigma, \quad (21)$$

$$v = 1/\sigma. \quad (22)$$

However, renormalization group analysis argues that the critical exponents take classical mean-field values in this region[43]. Although γ approaches 1, β is much larger than that in mean field model. Interestingly, the critical exponents of FePd₂Te₂ do not correspond to any conventional model, regardless of with long- or short-range interactions. A possible reason is that FePd₂Te₂ possesses different critical behavior below and above T_c , like the case in Pr_{0.6-x}Er_xCa_{0.1}Sr_{0.3}MnO₃[44], Cu₂OSeO₃[45] and FeGe[46]. The difference is that β is not close to any universal class.

To our best knowledge, the critical exponents of FePd₂Te₂ are the first set of values beyond conventional models in those of van der Waals magnets, which suggest the unconventional magnetic interactions and coupling. Due to

$$M_S(T) = M_0(-\varepsilon)^\beta, \varepsilon < 0, T < T_c, \quad (23)$$

$$\chi_0^{-1}(T) = (h_0/m_0)\varepsilon^\gamma, \varepsilon > 0, T > T_c, \quad (24)$$

γ and β reflect the divergence of inverse magnetic susceptibility above T_c and the growth speed of spontaneous magnetization below T_c , respectively. In FePd₂Te₂, the critical exponent γ close to 1 suggests a mean field model with isotropic long-range interactions above T_c . β with value 0.87 deviates from the prediction of the mean field model and is rather large. Such large β is never estimated in other van der Waals magnets, whose β is usually around 0.3[40]. Compared to those of other van der Waals magnets, δ of FePd₂Te₂ is also small. Such unconventional large β and small γ is also observed in doped manganites such as Ca_{0.85}Sm_{0.15}MnO₃[47], Ca_{0.85}Dy_{0.15}MnO₃[48] and Nd_{0.4}Sr_{0.6}MnO₃ nanoparticles[49].

Large value of β means slow growth of spontaneous magnetization, while small δ value results from the non-saturating behavior of field-dependent magnetization. The slow growth of spontaneous magnetization in FePd₂Te₂ can be attributed to measurement along c -axis, which is hard axis. Similar case occurs in Fe_{2.72}GeTe₂ with perpendicular magnetic anisotropy. In Fe_{2.72}GeTe₂, β along c -axis is 0.361(3), while 0.714(3) within ab -plane[50]. As for small δ , non-saturating behavior in other materials is usually attributed to an interface magnetism resulting in a current of spin-polarized electrons[51], little percent of antiferromagnetic phase[48], size-dependent ferromagnetism[49] and coexistence of non-ferromagnetic phases along with percolating ferromagnetic-clusters[52]. Also, finite-size ferromagnetic clusters in paramagnetic phases also leads to Griffiths phase, which is also one of the reasons for small

γ [47]. All these factors involve nano-structure in magnetic systems. In FePd₂Te₂, atomic twin boundary and in-plane anisotropy perpendicular to Fe chains lead to a natural antiferromagnetic component, which is responsible for non-saturating behavior. Fragmented Fe chains and magnetic clusters are also suggested. These results suggest the close relationship between the unusual critical exponents and structure in mesoscopic scale in FePd₂Te₂.

Although FePd₂Te₂ exhibits coercive field as high as 2.5 T, its T_c is only ~ 180 K, which is smaller than other van der Waals ferromagnets discovered recently, such as Fe₃GaTe₂[53]. In traditional theorem, finite-temperature long-range magnetic order is excluded in one-dimensional systems[54]. Finite T_c in FePd₂Te₂ can be attributed to two factors. One is that the Fe chains is nominally one-dimensional and actually kinked. The other is long-range magnetic interactions and interchain coupling. Thus, FePd₂Te₂ exhibits mean-field-like rather than one-dimensional ferromagnetism, although it crystallizes with quasi-one-dimensional Fe chains. In the same vein, enhancing interchain coupling is an effective way to increase T_c [55]. In metallic FePd₂Te₂, interchain coupling is mediated by itinerant electrons, so increasing carrier density through chemical doping in Pd/Te sites may be helpful. Electrostatic doping in devices based on thin flakes is not a good choice. Electrostatic doping usually requires small thickness down to few layers. However, the critical temperature T_c in thin flakes with spin-spin correlation exceeding the thickness will shift to lower temperatures than that of bulk[56]. For FePd₂Te₂ with long-range spin interactions, this means that the critical thickness is larger than those of other van der Waals ferromagnets, whose critical thickness is usually ~ 3 nm[57, 58].

IV. SUMMARY

In summary, influence of crystal twinning effect on electrical transport and magnetic properties are studied systematically. Easy-plane anisotropic orthorhombic crystal domains lead to natural antiferromagnetic coupling component near atomically sharp domain boundary and thus induce four-fold in-plane anisotropic magnetoresistance, which also reflects the pseudo four-fold lattice symmetry. The anisotropic magnetoresistance can be modulated by the fraction of domain boundary, thus by strain resulting from extra Pd atoms indirectly. Hopkinson effect observed in both AC and DC magnetic susceptibility indicates intense magnetic domain motion, which is rather rare in other van der Waals ferromagnets. Unusual critical exponents $\beta = 0.866$, $\gamma = 1.043$, $\delta = 2.20$ do not belong to any conventional universal class and evidence a decoupling between one-dimensional Fe-chains and mean-field-like ferromagnetism with long-range interactions. Large β and small γ is closely related to antiferromagnetic coupling component near crystal domain walls. These results also suggest the possible presence of fragmented Fe chains and magnetic clusters in

FePd₂Te₂. Twinning induced complicated spin texture, magnetic properties of detwinned FePd₂Te₂ and how to increase T_c are still needed further studied.

V. ACKNOWLEDGE

This work is supported by the National Natural Science Foundation of China (52250308) and the National Key Research and Development Program of China (2023YFA1406301). A portion of this work was carried out at the Synergetic Extreme Condition User Facility (SECUF).

-
- [1] S. Parsons, Introduction to Twinning, Acta Crystallographica Section D: Biological Crystallography **59**, 1995 (2003).
- [2] M. Nespolo, Tips and Traps on Crystal Twinning: How to Fully Describe Your Twin, Crystal Research and Technology **50**, 362 (2015).
- [3] I. R. Fisher, L. Degiorgi, and Z. Shen, In-plane Electronic Anisotropy of Underdoped ‘122’ Fe-Arsenide Superconductors Revealed by Measurements of Detwinned Single Crystals, Reports on progress in Physics **74**, 124506 (2011).
- [4] E. Specht, C. Sparks, A. Dhere, J. Brynstad, O. Cavin, D. Kroeger, and H. Oye, Effect of Oxygen Pressure on the Orthorhombic-Tetragonal Transition in the High-Temperature Superconductor YBa₂Cu₃O_x, Physical Review B **37**, 7426 (1988).
- [5] P. Radaelli, D. Hinks, A. Mitchell, B. Hunter, J. Wagner, B. Dabrowski, K. Vandervoort, H. Viswanathan, and J. Jorgensen, Structural and Superconducting Properties of La_{2-x}Sr_xCuO₄ as a Function of Sr content, Physical Review B **49**, 4163 (1994).
- [6] M. Tanatar, A. Kreyssig, S. Nandi, N. Ni, S. L. Bud’ko, P. Canfield, A. Goldman, and R. Prozorov, Direct Imaging of the Structural Domains in the Iron Pnictides AFe₂As₂ (A= Ca, Sr, Ba), Physical Review B—Condensed Matter and Materials Physics **79**, 180508 (2009).
- [7] R. Prozorov, M. Tanatar, N. Ni, A. Kreyssig, S. Nandi, S. Bud’ko, A. Goldman, and P. Canfield, Intrinsic Pinning on Structural Domains in Underdoped Single Crystals of Ba(Fe_{1-x}Co_x)₂As₂, Physical Review B—Condensed Matter and Materials Physics **80**, 174517 (2009).
- [8] S. Li, C. de La Cruz, Q. Huang, G. Chen, T.-L. Xia, J. Luo, N. Wang, and P. Dai, Structural and Magnetic Phase Transitions in Na_{1-δ}FeAs, Physical Review B—Condensed Matter and Materials Physics **80**, 020504 (2009).
- [9] T. McQueen, A. Williams, P. Stephens, J. Tao, Y. Zhu, V. Ksenofontov, F. Casper, C. Felser, and R. Cava, Tetragonal-to-Orthorhombic Structural Phase Transition at 90 K in the Superconductor Fe_{1.01}Se, Physical Review Letters **103**, 057002 (2009).
- [10] G. Dolan, G. Chandrashekar, T. Dinger, C. Feild, and F. Holtzberg, Vortex Structure in YBa₂Cu₃O₇ and Evidence for Intrinsic Pinning, Physical review letters **62**, 827 (1989).
- [11] I. Maggio-Aprile, C. Renner, A. Erb, E. Walker, and Ø. Fischer, Critical Currents Approaching the Depairing Limit at a Twin Boundary in YBa₂Cu₃O_{7-δ}, Nature **390**, 487 (1997).
- [12] C.-L. Song, Y.-L. Wang, Y.-P. Jiang, L. Wang, K. He, X. Chen, J. E. Hoffman, X.-C. Ma, and Q.-K. Xue, Suppression of Superconductivity by Twin Boundaries in FeSe, Physical Review Letters **109**, 137004 (2012).
- [13] C. Tsuei and J. Kirtley, Pairing Symmetry in Cuprate Superconductors, Reviews of Modern Physics **72**, 969 (2000).
- [14] T. Watashige, Y. Tsutsumi, T. Hanaguri, Y. Kohsaka, S. Kasahara, A. Furusaki, M. Sigrist, C. Meingast, T. Wolf, H. v. Löhneysen, *et al.*, Evidence for Time-Reversal Symmetry Breaking of the Superconducting State near Twin-Boundary Interfaces in FeSe Revealed by Scanning Tunneling Spectroscopy, Physical Review X **5**, 031022 (2015).
- [15] B. Shi, Y. Geng, H. Wang, J. Yang, C. Shang, M. Wang, S. Mi, J. Huang, F. Pan, X. Gui, *et al.*, FePd₂Te₂: An Anisotropic Two-Dimensional Ferromagnet with One-Dimensional Fe Chains, Journal of the American Chemical Society **146**, 21546 (2024).
- [16] G. Yang, J. Abell, P. Shang, I. Jones, and C. Gough, Growth and Microstructure in Bi₂Sr₂CaCu₂O_y Single Crystals, Journal of crystal growth **166**, 820 (1996).
- [17] J. K. Murthy and A. Venimadhav, 4f-3d Exchange Coupling Induced Exchange Bias and Field Induced Hopkinson Peak Effects in Gd₂CoMnO₆, Journal of Alloys and Compounds **719**, 341 (2017).
- [18] W. Tang, J. Liang, G. Rao, and X. Yan, Study of AC Susceptibility on the LaFe_{13-x}Si_x System, physica status solidi (a) **141**, 217 (1994).
- [19] G. Benka, A. Bauer, P. Schmakat, S. Säubert, M. Seifert, P. Jorba, and C. Pfleiderer, Interplay of Itinerant Magnetism and Spin-Glass Behavior in Fe_xCr_{1-x}, Physical Review Materials **6**, 044407 (2022).
- [20] N. Karma, D. Harinkhere, P. Karil, and H. Dager, Study of AC Susceptibility of La_{0.8}Sr_{0.2}MnO₃ at Different Frequencies, in *Journal of Physics: Conference Series*, Vol. 2603 (IOP Publishing, 2023) p. 012030.
- [21] D. Drobac, Critical Exponents from High-Precision AC Susceptibility Data, Journal of magnetism and magnetic materials **159**, 159 (1996).
- [22] A. Pramanik and A. Banerjee, Phase Separation and the Effect of Quenched Disorder in Pr_{0.5}Sr_{0.5}MnO₃, Journal of Physics: Condensed Matter **20**, 275207 (2008).
- [23] F. Li and J. Fang, Glassy-Ferromagnetic Behavior in Eu_{0.5}Sr_{0.5}CoO₃, Journal of magnetism and magnetic materials **324**, 2664 (2012).
- [24] J. K. Murthy, K. Chandrasekhar, H. Wu, H. Yang, J.-Y. Lin, and A. Venimadhav, Antisite Disorder Driven Spontaneous Exchange Bias Effect in La_{2-x}Sr_xCoMnO₆ (0 ≤ x ≤ 1), Journal of Physics: Condensed Matter **28**, 086003 (2016).

- [25] J. Sláma, M. Ušáková, M. Šoka, R. Dosoudil, and V. Jančárik, Hopkinson Effect in Soft and Hard Magnetic Ferrites, *Acta Physica Polonica A* **131**, 762 (2017).
- [26] S. U. Bhasker, G. Choudary, and M. R. Reddy, Modulation in Magnetic Exchange Interaction, Core Shell Structure and Hopkinson's Peak with Chromium Substitution into $\text{Ni}_{0.75}\text{Co}_{0.25}\text{Fe}_2\text{O}_4$ Nano Particles, *Journal of Magnetism and Magnetic Materials* **454**, 349 (2018).
- [27] P. Gaunt, S. Ho, G. Williams, and R. Cochrane, Critical Behavior of an Amorphous Ferromagnet, *Physical Review B* **23**, 251 (1981).
- [28] A. B. Pippard, *Magnetoresistance in Metals*, Vol. 2 (Cambridge university press, 1989).
- [29] R. Ramos, S. Arora, and I. Shvets, Anomalous Anisotropic Magnetoresistance in Epitaxial Fe_3O_4 Thin Films on MgO (001), *Physical Review B—Condensed Matter and Materials Physics* **78**, 214402 (2008).
- [30] Y. Ando, A. Lavrov, and S. Komiya, Anisotropic Magnetoresistance in Lightly Doped $\text{La}_{2-x}\text{Sr}_x\text{CuO}_4$: Impact of Antiphase Domain Boundaries on the Electron Transport, *Physical review letters* **90**, 247003 (2003).
- [31] X. Ma, M. Huang, S. Wang, P. Liu, Y. Zhang, Y. Lu, and B. Xiang, Anisotropic Magnetoresistance and Planar Hall Effect in Layered Room-Temperature Ferromagnet $\text{Cr}_{1.2}\text{Te}_2$, *ACS Applied Electronic Materials* **5**, 2838 (2023).
- [32] M. Bibes, B. Martinez, J. Fontcuberta, V. Trtik, C. Ferrater, F. Sánchez, M. Varela, R. Hiergeist, and K. Steenbeck, Anisotropic Magnetoresistance of (00h),(0hh) and (hhh) $\text{La}_{2/3}\text{Sr}_{1/3}\text{MnO}_3$ Thin Films on (001) Si Substrates, *Journal of magnetism and magnetic materials* **211**, 206 (2000).
- [33] M. Bibes, V. Laukhin, S. Valencia, B. Martinez, J. Fontcuberta, O. Y. Gorbenko, A. Kaul, and J. Martinez, Anisotropic Magnetoresistance and Anomalous Hall Effect in Manganite Thin Films, *Journal of Physics: Condensed Matter* **17**, 2733 (2005).
- [34] Y. Dai, Y. Zhao, L. Ma, M. Tang, X. Qiu, Y. Liu, Z. Yuan, and S. Zhou, Fourfold Anisotropic Magnetoresistance of Li_0FePt Due to Relaxation Time Anisotropy, *Physical Review Letters* **128**, 247202 (2022).
- [35] W. Eerenstein, T. Palstra, S. Saxena, and T. Hibma, Spin-Polarized Transport across Sharp Antiferromagnetic Boundaries, *Physical review letters* **88**, 247204 (2002).
- [36] P. Li, C. Jin, E. Jiang, and H. Bai, Origin of the Twofold and Fourfold Symmetric Anisotropic Magnetoresistance in Epitaxial Fe_3O_4 Films, *Journal of Applied Physics* **108** (2010).
- [37] D. Margulies, F. Parker, M. Rudee, F. Spada, J. Chapman, P. Aitchison, and A. Berkowitz, Origin of the Anomalous Magnetic Behavior in Single Crystal Fe_3O_4 Films, *Physical Review Letters* **79**, 5162 (1997).
- [38] A. Arrott and J. E. Noakes, Approximate Equation of State for Nickel near Its Critical Temperature, *Physical Review Letters* **19**, 786 (1967).
- [39] M. E. Fisher, The Theory of Equilibrium Critical Phenomena, *Reports on progress in physics* **30**, 615 (1967).
- [40] Q. H. Wang, A. Bedoya-Pinto, M. Blei, A. H. Dismukes, A. Hamo, S. Jenkins, M. Koperski, Y. Liu, Q.-C. Sun, E. J. Telford, *et al.*, The Magnetic Genome of Two-Dimensional van der Waals Materials, *ACS nano* **16**, 6960 (2022).
- [41] A. Pramanik and A. Banerjee, Critical Behavior at Paramagnetic to Ferromagnetic Phase Transition in $\text{Pr}_{0.5}\text{Sr}_{0.5}\text{MnO}_3$: A Bulk Magnetization Study, *Physical Review B—Condensed Matter and Materials Physics* **79**, 214426 (2009).
- [42] J. S. Kouvel and M. E. Fisher, Detailed Magnetic Behavior of Nickel near Its Curie Point, *Physical Review* **136**, A1626 (1964).
- [43] M. E. Fisher, S.-k. Ma, and B. Nickel, Critical Exponents for Long-Range Interactions, *Physical Review Letters* **29**, 917 (1972).
- [44] H. Omrani, M. Mansouri, W. C. Koubaa, M. Koubaa, and A. Cheikhrouhou, Critical Behavior Study near the Paramagnetic to Ferromagnetic Phase Transition Temperature in $\text{Pr}_{0.6-x}\text{Er}_x\text{Ca}_{0.1}\text{Sr}_{0.3}\text{MnO}_3$ ($x=0, 0.02$ and 0.06) Manganites, *RSC Advances* **6**, 78017 (2016).
- [45] H. C. Chauhan, B. Kumar, A. Tiwari, J. K. Tiwari, and S. Ghosh, Different Critical Exponents on Two Sides of a Transition: Observation of Crossover from Ising to Heisenberg Exchange in Skyrmion Host Cu_2OSeO_3 , *Physical Review Letters* **128**, 015703 (2022).
- [46] L. Zhang, H. Han, M. Ge, H. Du, C. Jin, W. Wei, J. Fan, C. Zhang, L. Pi, and Y. Zhang, Critical Phenomenon of the Near Room Temperature Skyrmion Material FeGe , *Scientific reports* **6**, 22397 (2016).
- [47] R. Nag, B. Sarkar, S. Pal, and E. Bose, Magnetic Properties and Critical Behavior of Electron Doped Polycrystalline $\text{Ca}_{0.85}\text{Sm}_{0.15}\text{MnO}_3$ Manganite, *Physica Scripta* **94**, 095801 (2019).
- [48] B. Sarkar, R. Nag, and S. Pal, Manifestation of Non-conventional Magnetic Interaction in Electron-Doped $\text{Ca}_{0.85}\text{Dy}_{0.15}\text{MnO}_3$ from Magnetic Properties and Critical Behavior Analysis, *Journal of Superconductivity and Novel Magnetism* **34**, 2059 (2021).
- [49] S. Kundu and T. Nath, Critical Behavior and Magnetic Relaxation Dynamics of $\text{Nd}_{0.4}\text{Sr}_{0.6}\text{MnO}_3$ Nanoparticles, *Philosophical Magazine* **93**, 2527 (2013).
- [50] W. Liu, Y. Wang, J. Fan, L. Pi, M. Ge, L. Zhang, and Y. Zhang, Field-Dependent Anisotropic Magnetic Coupling in Layered Ferromagnetic $\text{Fe}_{3-x}\text{GeTe}_2$, *Physical Review B* **100**, 104403 (2019).
- [51] K. Rumpf, P. Granitzer, and P. Pölt, Non-Saturating Magnetic Behaviour of a Ferromagnetic Semiconductor/Metal Nanocomposite, *Journal of magnetism and magnetic materials* **322**, 1283 (2010).
- [52] D. Kumar and A. Banerjee, A Critical Examination of Magnetic States of $\text{La}_{0.5}\text{Ba}_{0.5}\text{CoO}_3$: Non-Griffiths Phase and Interacting Ferromagnetic-Clusters, *arXiv preprint arXiv:1211.4936* (2012).
- [53] G. Zhang, F. Guo, H. Wu, X. Wen, L. Yang, W. Jin, W. Zhang, and H. Chang, Above-Room-Temperature Strong Intrinsic Ferromagnetism in 2d van der Waals Fe_3GaTe_2 with Large Perpendicular Magnetic Anisotropy, *Nature Communications* **13**, 5067 (2022).
- [54] N. D. Mermin and H. Wagner, Absence of Ferromagnetism or Antiferromagnetism in One-or Two-Dimensional Isotropic Heisenberg Models, *Physical Review Letters* **17**, 1133 (1966).
- [55] L. Duan, X. Wang, J. Zhang, Z. Hu, J. Zhao, Y. Feng, H. Zhang, H.-J. Lin, C. Chen, W. Wu, *et al.*, Synthesis, Structure, and Magnetism in the Ferromagnet La_3MnAs_5 : Well-Separated Spin Chains Coupled via Itinerant Electrons, *Physical Review B* **106**, 184405 (2022).
- [56] R. Zhang and R. F. Willis, Thickness-Dependent Curie Temperatures of Ultrathin Magnetic Films: Effect of the Range of Spin-spin Interactions, *Physical review letters*

- 86**, 2665 (2001).
- [57] Y. Deng, Y. Yu, Y. Song, J. Zhang, N. Z. Wang, Z. Sun, Y. Yi, Y. Z. Wu, S. Wu, J. Zhu, *et al.*, Gate-Tunable Room-Temperature Ferromagnetism in Two-Dimensional Fe_3GeTe_2 , *Nature* **563**, 94 (2018).
- [58] Z. Chen, Y. Yang, T. Ying, and J.-G. Guo, High- T_c Ferromagnetic Semiconductor in Thinned 3d Ising Ferromagnetic Metal Fe_3GaTe_2 , *Nano Letters* **24**, 993 (2024).